JPEG IMAGE COMPRESSION USING QUANTIZATION TABLE OPTIMIZATION BASED ON PERCEPTUAL IMAGE QUALITY ASSESSMENT

Yuebing Jiang and Marios S. Pattichis

University of New Mexico
Department of Electrical and Computer Engineering
Albuquerque, NM 87106

ABSTRACT

We consider the use of perceptual image quality assessment for quantization table (QT) optimization for JPEG compression. For evaluating performance, we consider the use of the Structural Similarity Index (SSIM) for evaluating distortion in the compressed images. This leads to the study of rate-SSIM curves that replace the traditional use of rate-distortion curves based on the PSNR.

We introduce a multi-objective optimization framework for estimating the best rate-SSIM curves. To estimate globally optimal quantization tables, A stochastic-optimization algorithm based on Simulated Annealing is proposed and its variations are studied.

We report results on all methods on the Lena image and results from selected methods on the LIVE image quality assessment database. For the LIVE database, compared to the use of the standard JPEG quantization table at quality factor QF=95, QTs based on the training set give average bitrate reductions of 11.68%, 7.7% and an increase of 2.4%, while the SSIM quality changes from $-0.11\%, +0.05\%$ and 0.12% respectively. In all cases, the results indicate that all considered methods improved over the use of standard JPEG tables.

Index Terms— Perception-based compression, JPEG, Simulated Annealing

1. INTRODUCTION

There is strong interest in the optimization of image compression method parameters based on objective methods for evaluating perceptual image quality. This renewed interest comes from the realization that the PSNR is a very poor measure of perceptual image quality [1, 2]. Thus, traditional rate-distortion curves based on PSNR cannot accurately reflect perceptually-optimal image compression. Instead, we consider the replacement of the PSNR by the Structural Similarity Index (SSIM) and the use of rate-SSIM curves for the evaluation of the performance of image compression methods (see [3] for SSIM).

This paper is focused on the development of a perception-motivated optimization method for still image compression.

Our focus is on developing a new optimization approach for estimating the best Discrete Cosine Transform (DCT) coefficient quantization tables. In terms of applications, our current focus is on the use of the optimal quantization tables with JPEG [4]. Here, we note that despite the introduction of the JPEG 2000 standard, JPEG remains the most common still image compression standard. However, it is important to note that our approach is very general and its extension to application with JPEG 2000 or other image and video compression methods should be straight-forward.

Some related work appears in [2]. In [2], the authors derived SSIM bounds as a function of the quantization rate for fixed-rate uniform quantization of image DCT coefficients, for high data rates. Here, we will consider rate-SSIM optimization for high SSIM index values. Similarly, the SSIM is used for the design of optimal linear equalizers in [1] and optimal linear restoration in [5].

The rest of the paper is organized as follows. We present a multi-objective optimization formulation in section 2. This is followed by the methodology in section 3. The results are presented in section 4, and concluding remarks are given in section 5.

2. A MULTI-OBJECTIVE OPTIMIZATION FORMULATION

We begin this section with a brief overview of the multi-objective optimization approach. We then discuss a stochastic optimization approach for solving the generated equations.

We consider the multi-objective optimization problem defined by

$$\min_{Q} \text{Rate}(Q, I), \quad \max_{Q} \text{SSIM}(Q, I) \qquad (1)$$

where I denotes the input image, $Q = (Q_1, \ldots, Q_{64})$ defines the Discrete Cosine Transform (DCT) quantization table parameters, Rate denotes the achieved bitrate in average bits per sample, SSIM(.) refers to the SSIM index. Here, the quantization table elements are integers with values from 1 to 255.

To solve Eq. (1), we need to find Pareto optimal points. Here, a solution is defined to be Pareto optimal if no other

feasible point can be found that has both a lower bitrate and a higher SSIM index. The set of solutions generated by this approach generates the rate-SSIM graph.

To estimate the Pareto optimal points, we consider a scalarization of Eq. (1), given by:

$$\max_{Q} \; \text{SSIM}\,(Q,\,I) - C_1 \text{Rate}(Q,\,I), \quad C_1 > 0 \quad (2)$$

Where C_1 denotes a scalar constant that provides for the relative weight between the conflicting objectives.

For initializing the optimization procedure, we will consider the standard JPEG quantization table defined in terms of the QF parameter. Thus, to generate the rate-SSIM graph, we will consider initializing the search at multiple values of the QF. Note that for each value of the QF, we also have corresponding initial values for the SSIM and $Rate$ index. This approach also provides for a method for estimating the scalar quantization parameter C_1. We estimate C_1 of Eq. (2) using central differencing:

$$C_1 \approx \frac{S_{QF_{i+1}} - S_{QF_{i-1}}}{R_{QF_{i+1}} - R_{QF_{i-1}}} \quad (3)$$

where $(S_{QF_{i+1}}, R_{QF_{i+1}})$ and $(S_{QF_{i-1}}, R_{QF_{i-1}})$ denote the initial SSIM and rate values for $QF = QF_{i+1}, QF_{i-1}$ respectively. It is interesting to note that Eq. (3) represents a slightly biased estimator since we expect the slope to increase as compared to standard JPEG.

Since the Quantization table is made up of integer values, we cannot consider Newton or other continuous-variable optimization method. Furthermore, due to the complexity of the search space, an integer programming approach will be intractable. Instead, we consider a global optimization approach based on Simulated Annealing(SA) [6].

3. METHODS

Simulated Annealing estimates the optimal value by forming a probability density function in terms of the function to be optimized. A Markov Chain of possible quantization table (QT) values is generated based on a transition probability defined between different QT values. The key to speed up convergence is to define an appropriate transition probability that will move the QT values closer to the optimal value in fewer iterations. Here, we will consider four different methods and then derive the transition probabilities for the most promising method.

In summary, we consider the following methods for generating the Markov Chain:

- Method 1: Uniformly choose the QT coefficient index i to modify. Then modify Q_i by $+1$ or -1 with equal probability.

- Method 2: Use a low-frequency exponential rule to select the QT coefficient index i to modify (low-frequencies selected more frequently). Then modify Q_i by $+1$ or -1 with equal probability.

- Method 3: Uniformly choose the QT coefficient index i to modify. Then modify Q_i by drawing a sample from a discrete Gaussian distribution with $\sigma = 1$.

- Method 4: Use a low-frequency exponential rule to select the QT coefficient index i to modify. Then modify Q_i by drawing a sample from a discrete Gaussian distribution with $\sigma = 1$.

- Method 5: Use a high-frequency exponential rule to select the QT coefficient index i to modify (high frequencies selected more frequently). Then modify Q_i by $+1$ or -1 with equal probability.

Method 1 is fairly straight-forward. Every possible neighbor is considered with equal probability, and the change between neighbors is with the smallest step. Methods 2, 4 and 5 use an exponential rule for deciding which QT coefficient should be changed next. To explain the exponential choice rule, let us consider the 8×8 DCT coefficient grid. We define the exponential choice rule based on:

$$f(i,\,j) = D \cdot \exp\left[-c(i+j)/15\right], i, j \in [1, \ldots, 8], \quad (4)$$

Where D is an appropriate normalization constant so that the discretized probabilities add up to 1. By abuse of notation, we thus select the $(i,\,j)$-th QT coefficient to modify based on $f(i,\,j)$. To return to the 1-D indices, simply map $(i,\,j)$ to the 1-D index given by $8(i-1) + j$. Furthermore, we map the 1-D index k to $(i,\,j)$ using $j = k \mod 8$ and $i = (k-j)/8 + 1$. We can use the exponential rule in (4) to encourage the selection of low-frequencies using c positive (methods 2 and 4 in section 4 use $c = 0.5$), or for encouraging the selection of high-frequencies using c negative,(method 5 in section 4 uses $c = -0.5$). In what follows, we let $f_E(.)$ denote the one-dimensional exponential distribution.

Method 3 allows for both small and larger changes in the QT coefficients based on a discretized Gaussian distribution. Method 4 combines the exponential rule of method 2 with the Gaussian changes of method 3. Method 5 is the same as method 2 but uses an exponential rule that verifies the selection of high-frequencies.

It can be shown that the use of the exponential rule in method 4 leads to the transition probability given by

$$f(Q^+, Q) = \sum_{i=1}^{i=64} \mathcal{N}_{Q_i^+}(\mu = Q_i, \sigma = 1) \cdot \delta(Q_i^+ = Q_i) \cdot f_E(i)$$

where Q denotes the current QT state, Q^+ denotes next state in the Markov Chain, $\mathcal{N}_{Q_i^+}$ denotes the one-dimensional discrete Gaussian distribution for the i-th coefficient of Q^+.

Fig. 1. Simulated Annealing (SA) Optimization for computing a Rate-SSIM optimal point.

Input: Image I, Quality Factor (QF), SA parameter C_0.
Output: Optimal quantization table Q.

1: Initialize Q to the standard JPEG quantization table for the specified quality factor QF. Compute the standard rate R_0 based on the optimal Huffman tables. Set $i = 1$.
2: Compute multi-objective parameter C_1 using Eq. (3).
3: Use method 1, 2, 3, 4, or 5 to select the next state Q^+ from the current state Q.
4: Compute the optimal Huffman table based on Q^+.
5: Compute the objective function O^+ based on Eq. (2).
6: Set $\lambda = C_0 * ln(1 + i)$, and decide whether to transition to Q^+ based on the transition probability defined by Eq. (5).
7: Set $i = i + 1$ for the next iteration.
8: Repeat 3 to 7 until i reaches the maximum number of iterations $MaxIterations$

Also, $\delta(Q_i^+ = Q_i)$ means that Q^+ keeps all of the coefficients of Q except for the i-th coefficient.

After generating the next state Q^+ from Q, the Simulated Annealing algorithm will jump to the next state with probability [6]:

$$min\{1, exp(\lambda \cdot (O^+ - O))\} \qquad (5)$$

where λ denotes a temperature parameter, O^+ represents the optimization function given by (2) evaluated at Q^+, and O represents (2) evaluated at Q.

The entire algorithm is summarized in Fig. 1. To generate the entire rate-SSIM graph, we need to run this algorithm for different values of the quality factor QF. For each value of QF, we may generate several Pareto-optimal points that outperform the standard JPEG QT.

4. RESULTS

We present results for the Lena image and the LIVE image quality database [7, 8]. We will first use the Lena image to discuss the proposed methods. Then, we provide a summary of the performance on the LIVE image quality database on methods 1, 2 and 5 in Tables 6, 7 and 8.

As described in the Methods section, we consider five different methods. We have results in Tables 1-5 from Methods 1-5 respectively. In all cases, we consider JPEG compression for the Lena image for Quality factor values: $QF = 85, 90, 95$ to initialize the search. Furthermore, we set the SA parameter at $C_0 = 5000$ for a maximum of 600 iterations. The final results are with the best object function evaluations during each iteration.

In Figures 2, 3, 4, we present the Pareto-optimal fronts for all 5 methods. In Fig. 2, we have the Pareto-optimal results

Table 1. Method 1 results for the Lena (512×512) image.

QF	Final rate	Final SSIM	Rate change	SSIM change
95	2.3717	0.9814	**-2.00%**	**0.36%**
90	1.5164	0.9621	-8.07%	-0.02%
85	1.2133	0.9523	-6.76%	-0.07%

Table 2. Method 2 results for the Lena (512×512) image based on the low-frequency exponential rule.

QF	Final rate	Final SSIM	Rate change	SSIM change
95	2.3036	0.9804	**-4.81%**	**0.25%**
90	1.5138	0.9617	-8.23%	-0.05%
85	1.1985	0.9524	-7.89%	-0.06%

Table 3. Method 3 results for the Lena (512×512) image based on discretized Gaussian model.

QF	Final rate	Final SSIM	Rate change	SSIM change
95	2.1843	0.9766	-9.74%	-0.13%
90	1.3341	0.9568	-19.12%	-0.56%
85	1.0812	0.9478	-16.90%	-0.55%

Table 4. Method 4 results for the Lena (512×512) image based on the low-frequency exponential rule and discretized Gaussian model.
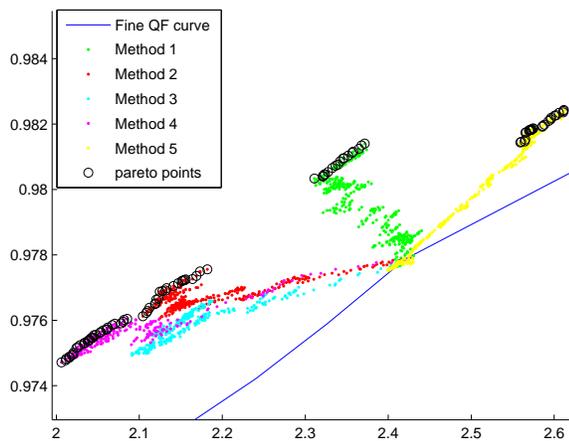
QF	Final Rate	Final SSIM	Rate change	SSIM change
95	2.0840	0.9759	-13.89%	-0.20%
90	1.3491	0.9575	-18.21%	-0.49%
85	1.0975	0.9486	-15.66%	-0.46%

Table 5. Method 5 results for the Lena (512×512) image based on the high-frequency exponential rule.

QF	Final Rate	Final SSIM	Rate change	SSIM change
95	2.6117	0.9824	7.92%	0.47%
90	1.6592	0.9626	0.59%	0.04%
85	1.3015	0.9531	0.02%	0.02%

for QF=95. Note that method 1 moves orthogonal to the original Rate-SSIM graph as intended. The rest of the methods either move above or below method 1. This trend seems to also occur in Figures 3 and 4. In Fig. 4, it is interesting to note that an entire, nearly-continuous Pareto front was generated from the use of the 5 methods for $QF = 85$. Overall, we select Methods 1, 2 and 5 to run with the LIVE database. Our choice is based on generating a diverse set of results as shown in Fig.2. In Fig. 2, it is clear that methods 2 and 5
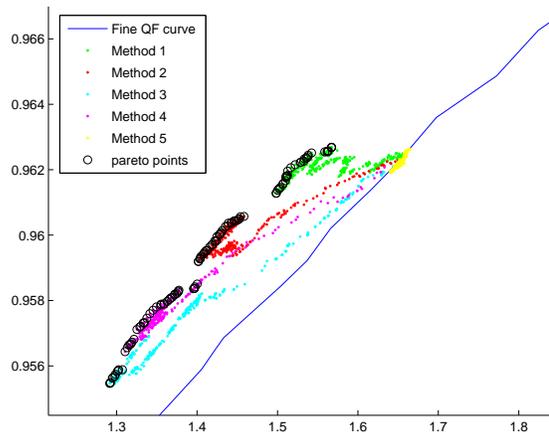
seem to go into different optimization directions. It is also interesting to note that method 2 favors low-frequency changes while method 5 favors high-frequency changes, while method 1 becomes the same as methods 2 and 5 for $c = 0$. It is easy to see that Method 1 is much better than the orginal standard QT since it produces a decrease in bitrate and an increase in the SSIM index. Method 2 can cause significant bitrate reduction, but this comes at a slight decrease in the SSIM index. Method 5 can lead to an increase in the SSIM index at a slightly increases bitrate, The methods using Gaussian models don't show significant difference from the methods using the exponential rule. Generally, by adjusting c in the exponential rule and C_1 in (2), the methods behave similarly. However, in all cases, the proposed methods yield improvements over the use of standard JPEG QTs (e.g., see Figs. 2-4).
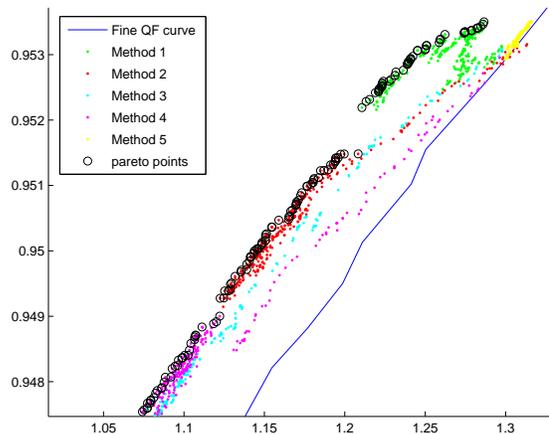

Fig. 3. Rate-SSIM comparisons for all methods for the Lena image for QF=90. The circled points represent Pareto-optimal results.

Fig. 2. Rate-SSIM comparisons for all methods for the Lena image at QF=95. The circled points represent Pareto-optimal results.

Fig. 4. Rate-SSIM comparisons for all methods for the Lena image at QF=85. The circled points represent Pareto-optimal results.

We use the leave one out method to test methods 1, 2 and 5 on the LIVE database. Here, we use 28 images for training and the remaining one for testing. In training, we compute the optimal quantization table for each one image and then take the median of all of them. During testing, the median quantization table is used on the remaining image. The results for methods 1, 2 and 5 are given in Tables 6 and 7 8 respectively.

From Table 6, it is clear that method 1 produced better results. The median quantization tables gave a rate decrease as well as an SSIM improvement. On average, we have a rate decrease of 7.7% and an SSIM increase of 0.06%. For method 2, we had an average rate decrease of 11.68% at a slight SSIM decrease of 0.11% (see Table 7). Method 5 emphasizes on SSIM improvement, with an average 0.12% increase of the SSIM, but also, the average bitrate increase 2.4%.

5. CONCLUSION

In this paper, we present a multi-objective optimization framework for JPEG image compression based on perceptual image quality assessment. In particular, we consider the use of rate-SSIM graphs for replacing the traditional use of rate-distortion graphs based on PSNR. As a particular example of this framework, we consider the optimization of the DCT coefficient quantization table.

For high quality factors, as compared to the use of the standard JPEG quantization tables, the optimized quantization tables form new rate SSIM curves that represent signif-

Table 6. Method 1 results for the LIVE database using leave one out validation on the median QT (QF=95). Here, we report the average, and the percentile results (min, 25th, 50th, 75th, max) on rate change.

File Name	Final Rate	Final SSIM	Rate change	SSIM change
Average			-7.70%	0.06%
'parrots'	1.5036	0.9817	-13.14% (min)	-0.09%
'sailing3'	2.1073	0.9802	-8.72% (25%)	0.06%
'sailing1'	2.7234	0.9885	-7.22% (50%)	0.07%
'cemetry'	3.3588	0.9910	-6.41% (75%)	0.11%
'building2'	4.2494	0.9953	-5.43% (max)	0.08%

Table 7. Method 2 results for the LIVE database using leave one out validation on the median QT (QF=95). Here , we report the average, and the percentile results (min, 25th, 50th, 75th, max) on rate change.

File Name	Final Rate	Final SSIM	Rate change	SSIM change
Average			-11.68%	-0.11%
'parrots'	1.4204	0.9802	-17.95% (min)	-0.24%
'womanhat'	2.1189	0.9799	-13.54% (25%)	-0.17%
'lighthouse2'	2.4562	0.9805	-11.28% (50%)	-0.14%
'woman'	3.0394	0.9829	-9.70% (75%)	-0.07%
'building2'	4.1291	0.9942	-8.10% (max)	-0.02%

Table 8. Method 5 results for the LIVE database using leave one out validation on the median QT (QF=95). Here, we report the average, and the percentile results (min, 25th, 50th, 75th, max) on rate change.

File Name	Final Rate	Final SSIM	Rate change	SSIM change
Average			2.40%	0.12%
'flowersonih35'	3.8631	0.9963	1.64% (min)	0.05 %
'bikes'	3.6631	0.9930	2.11% (25%)	0.10%
'rapids'	3.3482	0.9886	2.40% (50%)	0.17%
'lighthouse'	2.8465	0.984	2.62% (75%)	0.14%
'sailing2'	2.2470	0.978	3.39% (max)	0.17%

icant improvements. Our approach can also be extended to cover other image and video compression standards.

6. REFERENCES

[1] S.S. Channappayya, A.C. Bovik, C. Caramanis, and R.W. Heath, "Design of linear equalizers optimized for the structural similarity index," *IEEE Transactions on Image Processing,*, vol. 17, no. 6, pp. 857 –872, 2008.

[2] S.S. Channappayya, A.C. Bovik, and R.W. Heath, "Rate bounds on ssim index of quantized images," *IEEE Trans-actions on Image Processing,*, vol. 17, no. 9, pp. 1624 –1639, 2008.

[3] Zhou Wang, A.C. Bovik, H.R. Sheikh, and E.P. Simon-celli, "Image quality assessment: from error visibility to structural similarity," *IEEE Transactions on Image Processing,*, vol. 13, no. 4, pp. 600 –612, 2004.

[4] William B. Pennebaker and Joan L. Mitchell, *JPEG Still Image Data Compression Standard*, Kluwer Academic Publishers, Norwell, MA, USA, 1st edition, 1992.

[5] S.S. Channappayya, A.C. Bovik, C. Caramanis, and R.W. Heath, "Ssim-optimal linear image restoration," in *IEEE International Conference on Acoustics, Speech and Signal Processing, 2008. ICASSP 2008.*, 312008-april4 2008, pp. 765 –768.

[6] Sheldon M.Ross, *Simulation(Third Edition)*, Academic Press, 2002.

[7] L. Cormack H.R. Sheikh, Z.Wang and A.C. Bovik, "Live image quality assessment database release 2," .

[8] H.R. Sheikh, M.F. Sabir, and A.C. Bovik, "A statistical evaluation of recent full reference image quality assessment algorithms," *IEEE Transactions on Image Processing,*, vol. 15, no. 11, pp. 3440 –3451, 2006.